Generalized methodology for thermal diffusivity depth profile reconstruction in semi-infinite and finitely thick inhomogeneous solids

Andreas Mandelis, Frank Funak, and Mahendra Munidasa[a)]
Department of Mechanical and Industrial Engineering, University of Toronto, 5 King's College Road, Toronto, Ontario M5S 3G8, Canada and Manufacturing Research Corporation of Ontario, 1075 North Service Road West, Suite 201, Oakville, Ontario L6M 2G2, Canada

(Received 29 May 1996; accepted for publication 13 August 1996)

The formulation of a generalized expression for the thermal-wave field in an inhomogeneous finite-thickness solid on a homogeneous semi-infinite substrate is discussed. This is based on the Hamilton–Jacobi formulation of the thermal-wave problem [A. Mandelis, J. Math. Phys. **26**, 2676 (1985)]. An algorithm to invert simulated photothermal frequency scan data in obtaining thermal diffusivity profiles using this expression is reported. The tolerance of this inversion procedure to noise in both simulated and experimental data is also discussed. © *1996 American Institute of Physics.* [S0021-8979(96)02122-6]

I. INTRODUCTION

Among the modern-day nondestructive evaluation (NDE) methodologies, thermal-wave detection[1] is a technique growing in importance due to its ability to monitor subsurface structures and damage in materials, well beyond the optical penetration depth of illumination sources, i.e., below the range of optical imaging for opaque materials. The amplitude and phase of the thermal wave generated by an optical or other thermal energy source at the surface of an opaque material are detected either in the back-scattering or in transmission mode using a variety of sensor probes. In inhomogeneous materials, these two thermal-wave signal channels carry information about any heat transport disruption or change below the surface, which must be interpreted with appropriate models in order to yield reliable reconstructions of the spatially variant thermal diffusivity of the sample.

One of the first theories of this kind of inversion was described by Vidberg *et al.*[2] This model pertains to the thermal-wave surface signal obtained by measuring the radial variation of the surface temperature of a continuously inhomogeneous solid about a heated point at a single modulation frequency. Both thermal conductivity and heat capacity profiles were reconstructed using Padé approximants for the inversion of spatial Laplace transforms. There is a number of constraints that limits the applicability of this model. The most significant ones are (1) it is only valid for a nonconventional experimental geometry; (2) the reconstructed profiles are not always numerically reliable; (3) the accuracy is limited to a depth reconstruction on the order of one thermal diffusion length; and (4) the reconstruction algorithm is relatively complex and is sensitive to small amounts of error. In an earlier publication Jaarinen and Luukkala[3] discussed a numerical analysis of the same experimental geometry based on the solution of the thermal-wave equation at a single modulation frequency. The analysis uses a two-dimensional finite difference grid.

More recently, another major attempt[4] was made to approach the thermal-wave inverse problem more rigorously and for more general geometries than foregoing papers. In this approach the well-known Hamilton–Jacobi formalism from classical mechanics was introduced into the thermal-wave problem by treating the ac temperature field as a thermal harmonic oscillator (THO)[5] and inverting the amplitude and phase of the experimental data through matching to explicit theoretical expressions for a semi-infinite solid (or liquid). The first experimental inversions were obtained from the liquid crystal octylcyanobiphenyl (8CB)[6] using this method. Further inversions with semi-infinite laser-processed solids were reported later.[7,8] An inversion procedure for a finite thickness problem was also reported based on the same THO approach.[5] More recently, a newer model[9] motivated by the approach described by Mandelis and co-workers[4–8,10] was proposed, that assumed locally constant or linearly-dependent thermal conductivity on depth. In that work the solid was divided up into a virtual incremental discrete-layer system and in each layer forward and reverse thermal-wave equations were set up for constant conductivity and solved using computer-based matrix routines. The resulting equations were inverted for the depth-dependent increments of the value of the thermal conductivity using a commercially available nonlinear least-squares fit routine. It is well established that only true material discontinuities such as surfaces and not virtual incremental slices can generate reflected thermal waves. This raises questions about the validity and/or uniqueness of the inversions. Even if it is accurate for semi-infinite solids, the theory presents problems with the treatment of finite-thickness materials, as it ignores the multiple interreflections of the thermal wave between the two boundaries (surfaces) of the material. Fivez and Thoen reported yet another version[11] of the foregoing inversion problem with a linear dependence of the local (incremental) thermal conductivity with depth. Explicit expressions were derived and matched with experimental data and the results of the inversions were in good agreement with those obtained by the approach by Ma *et al.*[7] The major shortcoming of this new approach is in its inability to treat semi-infinite solids, since the explicit formulas depend on the boundedness of the derived Bessel and Neumann functions. Instead, their method[11] requires flat profiles in the bulk of the material under investigation. This is so because many of the combinations of

a)Electronic mail: munidasa@me.utoronto.ca

 0021-8979/96/80(10)/5570/9/$10.00

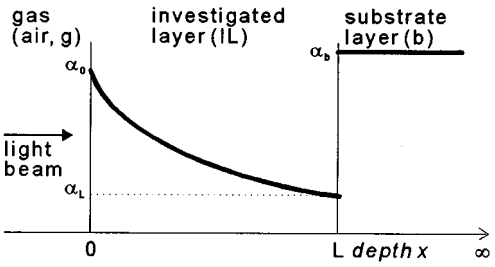

FIG. 1. An illustration of the relationship between depth vs thermal diffusivity for a test sample having an investigation layer of arbitrary thermal diffusivity profile, and a substrate layer.

these functions utilized in this approach become infinite in value as the depth increases without bound. A very recent theoretical approach by Lan *et al.*[12] combines the approaches of two prior papers.[9,11] Therefore, it has improved strengths, yet it is subject to some combinations of their shortcomings: a flat profile of the thermal conductivity at large distances[13] (i.e., at ''infinity''), to induce boundedness, along with the lack of a theoretical basis to treat multiple thermal-wave reflections from the opposite surfaces of finitely thick samples. In a most recent theoretical paper[14] Fivez and Thoen presented a new analytical approach to the inverse problem that is valid for semi-infinite solids at sufficiently high frequencies, but shows significant deviations of reconstructed thermophysical profiles from the expected values at low frequencies (equivalent to large depths in a sample).

In this article we formulate a complete generalized expression for the thermal-wave field in an inhomogeneous solid bounded by regions such as those shown in Fig. 1. This expression can be used for the semi-infinite case just by taking the limit $L\rightarrow\infty$. The formulas derived previously[4,7,10] based on the THO approach were adequate for the specific geometries dealt with in those cases, but were found to have several shortcomings. Those derived for the continuously inhomogeneous *semi-infinite* sample in Refs. 4 and 7 do not converge to the appropriate limits at low frequencies. Also, the *finite-thickness problem* reported in Ref. 10 does not converge to the homogeneous limit smoothly.

II. THEORY

A. Semi-infinite inhomogeneous solid

From the Hamilton–Jacobi treatment of thermal-wave physics as a thermal harmonic oscillator,[5] for the ac temperature field generated by a modulated energy source (e.g., a laser beam) in the material with a distributed thermal diffusivity $\alpha(x)$ one may write

$$T_s(x)=\frac{1}{2\sqrt{e(x)}}\left(\frac{p_{\tau_0}}{\sqrt{\omega}}\exp(-i\pi/4)+\tau_0\right)\exp[H(x)]$$
$$-\frac{1}{2\sqrt{e(x)}}\left(\frac{p_{\tau_0}}{\sqrt{\omega}}\exp(-i\pi/4)-\tau_0\right)$$
$$\times\exp[-H(x)];\quad 0\leqslant x\leqslant\infty, \tag{1}$$

where ω is the angular modulation frequency of the laser intensity where one-dimensional heat flow is assumed. The local thermal effusivity $e(x)$ of the solid at a depth x is defined as

$$e(x)=\sqrt{k(x)\rho(x)c(x)}. \tag{2}$$

Here k, ρ, and c are thermal conductivity, density, and specific heat, respectively. The exponent

$$H(x)=\int_0^x\sigma_s(y,\omega)dy, \tag{3}$$

where σ_s is defined as

$$\sigma_s(y,\omega)=(1+i)\sqrt{\frac{\omega}{2\alpha_s(y)}}, \tag{4}$$

where $\alpha_s(y)$ is the thermal diffusivity distribution of the solid at $x=y$ and $p_{\tau 0}$ and τ_0 are constants of integration and can be determined by boundary and limiting conditions. The material under investigation is assumed to be opaque.

In the limit $x\rightarrow\infty$, the ac temperature, $T(x)$, generated by the modulated laser should be zero. Applying this condition to Eq. (1) yields

$$p_{\tau_0}=-\sqrt{\omega}\,\exp(i\pi/4)\,\tau_0\left(\frac{1+\exp[-2H(\infty)]}{1-\exp[-2H(\infty)]}\right). \tag{5}$$

At the interface $x=0$, a net nonzero incident (photo) thermal heat flux is assumed:

$$-k_s\frac{d}{dx}T_s(x)\bigg|_{x=0}=\frac{1}{2}Q_0, \tag{6}$$

where Q_0 represents the thermal source fluence at the material surface [W/m^2] assuming 100% laser power absorption. Differentiating Eq. (1) and substituting in Eq. (6) gives

$$-p_{\tau_0}\sqrt{e(0)}+\frac{\tau_0\alpha(0)e'(0)}{2\sqrt{e(0)}}=\frac{Q_0}{2}. \tag{7}$$

Substituting Eq. (5) in Eq. (7) gives

$$\tau_0\approx\frac{Q_0}{2\sqrt{\omega}\,\exp(i\pi/4)\sqrt{e(0)}}\left(\frac{1-\exp[-2H(\infty)]}{1+\exp[-2H(\infty)]}\right). \tag{8}$$

In deriving Eq. (8) an approximation was made in neglecting a flux component due to a second-order effect, namely, the derivative of the thermal effusivity $e(x)$ was set equal to zero:

$$e'(0)=\frac{d}{dx}e(x)\bigg|_{x=0}\approx 0. \tag{9}$$

This assumption amounts to a requirement for nonsteep local variations of the effusivity; it is easily satisfied when the thermophysical field is evaluated at small incremental depth slices where it is not expected that local steep diffusivity gradients may exist.

Substituting Eqs. (5) and (8) in Eq. (1) gives

$$T(x)=\frac{Q_0R^{1/2}(x)}{2\sigma(0)k(0)}\left(\frac{1-\exp\{-2[H(\infty)-H(x)]\}}{1+\exp[-2H(\infty)]}\right)\times\exp[-H(x)], \tag{10}$$

where

$$R(x)=\frac{e(0)}{e(x)}. \tag{10a}$$

Equation (10) is the full expression for the thermal-wave field in an inhomogeneous solid, therefore, in what follows, the subscript ''in'' will be used to indicate this fact. This expression, however, does not adequately satisfy all possible boundary conditions in composite (two-layer) solids.

In formulating a complete expression for the thermal-wave field in an inhomogeneous solid bounded by regions such as those shown in Fig. 1 ($L\to\infty$, in this case), the concept of linear superposition of solutions of the heat-conduction (thermal-wave) differential equation will be invoked: according to this principle, any complicated linear boundary-value problem can have a solution written as a linear combination of solutions to a number of simpler boundary-value problems, so as to fully satisfy all boundary conditions of the original problem. In the present case, the group of simpler equations required to satisfy all boundary conditions of the problem of Fig. 1 consists of all the equations (and their solutions) valid for the various constant, variable, and limiting values of thermophysical properties of the geometry. Although it will be seen that the results are valid for arbitrary thermal diffusivity depth profiles, for this analysis let us assume a simple simulated functional dependence of the solid thermal diffusivity in the form,

$$\alpha_s(x)=\alpha_0\left(\frac{1+\Delta e^{-qx}}{1+\Delta}\right)^2, \tag{11a}$$

such that $\alpha_s(\infty)=\alpha_\infty$, $\alpha_s(0)=\alpha_0$ and

$$\Delta=\sqrt{\alpha_0/\alpha_\infty}-1, \tag{11b}$$

where $\alpha_0>\alpha_\infty$. The parameter q is a constant that determines the rate of thermophysical decay.

Insertion of the above two equations in the integral for $H(x)$, Eq. (3), gives $H(\infty)\to\infty$. Therefore, the temperature field in the inhomogeneous field from Eq. (10) is

$$T_{\rm in}(x)=\frac{Q_0R^{1/2}(x)}{2\sigma_0k_0}\exp[-H(x)], \tag{12}$$

where $\sigma(0)=\sigma_0$ and $k(0)=k_0$. The boundary values of the diffusivity involved inside the solid are α_0 and α_∞. The air–solid interface will not be considered, because in most practical cases the thermal coupling coefficient $R_{\rm air,0}\ll 1$ (near adiabatic conditions). The other thermal-wave fields represented in Fig. 1 ($L\to\infty$), are

$$T_0(x)=\frac{Q_0}{2\sigma_0k_0}e^{-\sigma_0x} \tag{13a}$$

and

$$T_\infty(x)=\frac{Q_0}{2\sigma_\infty k_\infty}e^{-\sigma_\infty x}, \tag{13b}$$

with constant diffusivities α_0 and α_∞, respectively. Now using the superposition principle, the general solution of the thermal-wave field in the solid can be written

$$T(x)=aT_{\rm in}(x)+bT_0(x)+cT_\infty(x), \tag{14}$$

where a, b, and c are constants to be determined by the various limiting case requirements of the problem.

B. Determination of the constants (a,b,c) and limiting cases

1. At large distances compared to the inhomogeneous region: $x\to\infty$

Since Eq. (11) gives a constant diffusivity profile of α_∞ at very large distances from the surface, $T(x,\omega)=T_\infty(x,\omega)$ in this limit. Therefore, Eq. (14) leads to

$$\lim_{x\to\infty}\left\{a\left(\frac{T_{\rm in}(x,\omega)}{T_\infty(x,\omega)}\right)+b\left(\frac{T_0(x,\omega)}{T_\infty(x,\omega)}\right)+c\right\}=1. \tag{15}$$

Substituting Eqs. (12), (13a), and (13b) in Eq. (15)

$$aR^{1/2}(\infty)\,\frac{e_\infty}{e_0}\exp\{\lim_{x\to\infty}[\sigma_\infty x-H(x)]\}+b\,\frac{e_\infty}{e_0}\exp\{\lim_{x\to\infty}[-(\sigma_0-\sigma_\infty)x]\}+c=1. \tag{16}$$

Since $\alpha_0>\alpha_\infty$ (i.e., $|\sigma_0|<|\sigma_\infty|$), the second term in Eq. (16) will become infinite. Therefore, to avoid that we can set $b=0$. It can be shown that[4]

$$\exp\{\lim_{x\to\infty}[\sigma_\infty x-H(x)]\}=\exp(\sigma_\infty J_\infty), \tag{17}$$

where

$$J_\infty=\frac{1}{2q}\ln\left(\frac{\alpha_0}{\alpha_\infty}\right). \tag{18}$$

Equations (16)–(18) lead to

$$a=(1-c)\,\frac{R_\infty}{\sqrt{R(\infty)}}\exp(-\sigma_\infty J_\infty). \tag{19}$$

2. Very high frequencies: $\omega\to\infty$

In this limit the penetration depth of the thermal wave is zero, hence the following limit is valid:

$$T(0,\omega\to\infty)=T_0(0,\omega). \tag{20}$$

Substituting Eqs. (13a), (13b), (19), (20), and $b=0$ in Eq. (14), and since $\sigma_\infty\to\infty$ in the limit $\omega\to\infty$, it can be shown that

$$c=\frac{T_0(0,\omega)}{T_\infty(0,\omega)}=\frac{k_\infty\sigma_\infty}{k_0\sigma_0}=\frac{1}{R_\infty}. \tag{21}$$

3. Very low frequencies: $\omega\to 0$

Since the penetration depth is infinite in this limit

$$T(0,\omega\to 0)=T_\infty(0,\omega). \tag{22}$$

Substituting Eqs. (20), (21), and $b=0$ in Eq. (14), and since $\sigma_\infty\to 0$ in the limit $\omega\to 0$, it can be shown that

$$\left(1-\frac{1}{R_\infty}\right)\frac{R_\infty}{\sqrt{R(\infty)}}=R_\infty-1$$

$$\therefore R(\infty)=1. \tag{23}$$

Finally, substituting all the determined constants from Eqs. (21), (23), and T_0, T_∞ from Eqs. (13a) and (13b) at $x=0$ in Eq. (14), the surface temperature of a semi-infinite inhomogeneous medium is

$$T(0,\omega)=\frac{Q_0}{2\sigma_0 k_0}\left[1+(R_\infty-1)\exp(-\sigma_\infty J_\infty)\right]. \tag{24}$$

C. Solid of finite thickness on homogeneous substrate

Here, Eq. (1) represents the ac temperature field in the region $0\leqslant x\leqslant L$. The constants $p_{\tau 0}$ and τ_0 can be determined by boundary and limiting conditions.

At the interface $x=0$ the boundary condition Eq. (6) is assumed. At the interface $x=L$, continuity of heat flux and temperature are assumed as

$$k_s\frac{d}{dx}T_s(x)\bigg|_{x=L}=k_b\frac{d}{dx}T_b(x)\bigg|_{x=L}, \tag{25a}$$

$$T_s(L)=T_b(L), \tag{25b}$$

where $T_s(x)$ is given by Eq. (1) in the region of $0\leqslant x\leqslant L$, and $T_b(x)$ is the temperature field in the semi-infinite bulk given by

$$T_b(x)=\frac{Q_0}{2\sigma_b k_b}\exp[-\sigma_b(x-L)]. \tag{26}$$

Differentiating Eq. (1), substituting in Eq. (6), and evaluating at $x=0$ yields

$$p_{\tau_0}=-\frac{Q_0}{2\sqrt{e(0)}}. \tag{27}$$

In deriving Eq. (27) the same approximation, $de(x)/dx=0$, discussed earlier, has been made. Similarly, evaluating Eq. (25a) at $x=L$ and then substituting for $p_{\tau 0}$ from Eq. (27) gives the following expression:

$$\tau_0=\frac{Q_0 e^{-i\pi/4}}{2\sqrt{e(0)\omega}}\left(\frac{1+\gamma_{b(L)}e^{-2H(L)}}{1-\gamma_{b(L)}e^{-2H(L)}}\right), \tag{28}$$

where

$$\gamma_{b(L)}\equiv\frac{1-R_{b(L)}}{1+R_{b(L)}};\quad R_{b(L)}\equiv\frac{e_b}{e(L)}, \tag{29}$$

and e_b, $e(L)$ represent the thermal effusivities, respectively, at the top of the substrate layer (which is assumed to have constant thermophysical properties), and at the directly adjacent and contacting bottom of the solid material layer with variable thermophysical properties. Finally, using Eq. (1) with the derived values of the parameters τ_0 and $p_{\tau 0}$ gives an expression for the thermal-wave field in the inhomogeneous solid:

$$T_{\text{in}}(x)=\frac{Q_0\sqrt{R(x)}}{2\sigma(0)k(0)}\left(\frac{1+\gamma_{b(L)}e^{-2[H(L)-H(x)]}}{1-\gamma_{b(L)}e^{-2H(L)}}\right)e^{-H(x)}, \tag{30}$$

where $R(x)$ was defined in Eq. (10a) and $\sigma(x)$ was defined in Eq. (4).

Now let us assume a simple simulated functional dependence of the solid thermal diffusivity in the form of Eq. (11a) for the region bounded by $x=0$ and $x=L$, such that $\alpha_s(L)=\alpha_L$, $\alpha_s(0)=\alpha_0$, and

$$\Delta=\frac{1-\sqrt{\alpha_L/\alpha_0}}{\sqrt{\alpha_L/\alpha_0}-e^{-qL}}. \tag{31}$$

Insertion of the above equation and Eq. (11a) in the integral for $H(L)$, Eq. (3), yields

$$H(L)=(1+i)\sqrt{\frac{\omega}{2\alpha_L}}\left(\frac{1-e^{-qL}}{1-\sqrt{(\alpha_0/\alpha_L)e^{-qL}}}\right)\times\left[L-\frac{1}{2q}\ln\left(\frac{\alpha_0}{\alpha_L}\right)\right]. \tag{32}$$

Therefore, the boundary values of the diffusivity involved inside the solid are α_0 and α_L.

The air–solid interface will be considered to be adiabatic as discussed before. The various thermal-wave fields represented in Fig. 1, with the definition of $\alpha_s(x)$ given by Eq. (11a) and Eq. (31), are

$$T_0(x)=\frac{Q_0}{2\sigma_0 k_0}\left(\frac{1+\gamma_{b0}e^{-2\sigma_0(L-x)}}{1-\gamma_{b0}e^{-2\sigma_0 L}}\right)e^{-\sigma_0 x}, \tag{33}$$

$$T_L(x)=\frac{Q_0}{2\sigma_L k_L}\left(\frac{1+\gamma_{bL}e^{-2\sigma_L(L-x)}}{1-\gamma_{bL}e^{-2\sigma_L L}}\right)e^{-\sigma_L x}, \tag{34}$$

where

$$\gamma_{bL}\equiv\frac{1-R_{bL}}{1+R_{bL}};\quad R_{bL}\equiv\frac{e_b}{e_L}. \tag{34a}$$

The backing material is also involved in terms of the thermal coupling coefficient at the interface $x=L$, therefore, the form of the thermal-wave field due to the backing is also required [Eq. (26)]. Now, using the superposition principle, the general solution of the thermal-wave field in the finite solid can be written

$$T(x)=aT_{\text{in}}(x)+bT_0(x)+cT_L(x), \tag{35}$$

where a, b, and c are constants to be determined by the various limiting case requirements of the problem.

D. Determination of the constants (a,b,c) and limiting cases

1. At the interface: $x\to L$

In this limit $T(x\to L)\to T_b(L)$. Evaluating Eq. (35) at $x=L$ and dividing by $T_b(L)$ from Eq. (26), renders the value of this ratio equal to 1 according to the boundary condition Eq. (25b). This gives an equation among the constants (a,b,c); solving for a yields

$$a=\frac{R_b}{\sqrt{R}(L)}\left[1-\frac{b}{R_b}\left(\frac{1+\gamma_{b0}}{1-\gamma_{b0}e^{-2\sigma_0 L}}\right)e^{-\sigma_0 L}-c\,\frac{R_L}{R_b}\left(\frac{1+\gamma_{bL}}{1-\gamma_{bL}e^{-2\sigma_L L}}\right)e^{-\sigma_L L}\right]\times\left(\frac{1-\gamma_{b(L)}e^{-2H(L)}}{1+\gamma_{b(L)}}\right)e^{H(L)}. \tag{36}$$

Substituting back into Eq. (35) the value of a above gives

$$T(0)=\Theta_0(\omega)\left\{\frac{R_b}{\sqrt{R(L)}}\left(\frac{1+\gamma_{b(L)}e^{-2H(L)}}{1+\gamma_{b(L)}}\right)\times\left[1-b\,\frac{1}{R_b}\left(\frac{1+\gamma_{b0}}{1-\gamma_{b0}e^{-2\sigma_0 L}}\right)e^{-\sigma_0 L}-c\,\frac{R_L}{R_b}\left(\frac{1+\gamma_{bL}}{1-\gamma_{bL}e^{-2\sigma_L L}}\right)e^{-\sigma_L L}\right]e^{H(L)}+b\left(\frac{1+\gamma_{b0}e^{-2\sigma_0 L}}{1-\gamma_{b0}e^{-2\sigma_0 L}}\right)+cR_L\left(\frac{1+\gamma_{bL}e^{-2\sigma_L L}}{1-\gamma_{bL}e^{-2\sigma_L L}}\right)\right\}, \tag{37}$$

where the following definition was made:

$$\Theta_0(\omega)\equiv\frac{Q_0}{2\sigma_0 k_0}, \tag{38}$$

reminiscent of the thermal-wave field at the surface of a solid with (constant) thermophysical properties α_0 and k_0.

2. Very high frequency limit: $\omega\to\infty$

In the limit of very high laser-beam-intensity modulation frequency ($\omega\to\infty$) the thermal wave probes only the surface. Therefore, $T(0,\omega\to\infty)\to\Theta_0(\omega)$. In this limit, Eq. (32) shows that $H(L)\to\infty$. Therefore, to keep the expression in Eq. (37) finite as ω increases without bound, one sets

$$de^{H(L)}=1+\gamma_{b(L)}. \tag{39}$$

Here, d is another constant to be evaluated. Substituting Eq. (39) in Eq. (37) yields

$$T(0)=\Theta_0(\omega)\,\frac{R_b}{d\sqrt{R(L)}}\,(1+de^{-H(L)}-e^{-2H(L)})\times\left[1-b\,\frac{1}{R_b}\left(\frac{1+\gamma_{b0}}{1-\gamma_{b0}e^{-2\sigma_0 L}}\right)e^{-\sigma_0 L}-c\,\frac{R_L}{R_b}\left(\frac{1+\gamma_{bL}}{1-\gamma_{bL}e^{-2\sigma_L L}}\right)e^{-\sigma_L L}\right]+\Theta_0(\omega)\times\left[b\left(\frac{1+\gamma_{b0}e^{-2\sigma_0 L}}{1-\gamma_{b0}e^{-2\sigma_0 L}}\right)+cR_L\left(\frac{1+\gamma_{bL}e^{-2\sigma_L L}}{1-\gamma_{bL}e^{-2\sigma_L L}}\right)\right]. \tag{40}$$

3. Semi-infinite limit: $L\to\infty$

Equation (40) should remain bounded as $L\to\infty$, yielding the expression Eq. (24) for the semi-infinite solid. As $L\to\infty$, then $H(L)\to\infty$. Now, making the following definition

$$\sigma_L L-H(L)\equiv\sigma_L J_L \tag{41}$$

gives

$$J_L=\frac{1}{1-\sqrt{\alpha_0/\alpha_L}e^{-qL}}\left((1-\sqrt{\alpha_0/\alpha_L})Le^{-qL}+\frac{1}{2q}\,(1-e^{-qL})\ln(\alpha_0/\alpha_L)\right). \tag{42}$$

In the limit of very large L, Eq. (42) becomes identical to Eq. (18), as expected,

$$J_L(\infty)\equiv\frac{1}{2q}\,\ln(\alpha_0/\alpha_L)=J_\infty. \tag{43}$$

As stated above, when $L\to\infty$, Eq. (40) must conform with Eq. (24) for the semi-infinite solid. Thus, in the limit $L\to\infty$, the right-hand sides of Eqs. (40) and (24) must be equal:

$$\frac{R_b}{d\sqrt{R(L)}}+b+cR_L\equiv 1+(R_L-1)e^{-\sigma_L J_L(\infty)}. \tag{44}$$

At this stage two more equations are required to relate constants d, b, and c. These can be obtained in the following limits.

4. The very low frequency limit: $\omega\to 0$

In this case it can be shown that

$$H(L)\sim J_L(L)\to 0. \tag{45}$$

Since the thermal diffusion length becomes infinite at $\omega\to 0$, the effect of the investigated layer becomes negligible. Therefore

$$T(0)\to\frac{Q_0}{2k_b\sigma_b}=T_b(0,\omega). \tag{46}$$

Equating the right-hand side of Eq. (40) in the limit $\omega\to 0$ to Eq. (46) yields

$$\left(1-\frac{1}{\sqrt{R(L)}}\right)(b+c-1)=0. \tag{47}$$

Since the main purpose here is to solve for b and c, let us choose

$$b+c-1=0. \tag{48}$$

Substituting for b in Eq. (44) gives

$$\frac{R_b}{d\sqrt{R(L)}}=(R_L-1)(e^{-\sigma_L J_L}-c). \tag{49}$$

5. Homogeneous limit: $\alpha(x)=\alpha_0=\alpha_L=$ constant

In this case $R_L=1$. Inserting this result into the updated version (with $b=1-c$) of Eq. (40) results in the following simplified expression:

$$T(0,L,\omega)=\Theta_0(\omega)\left(\frac{1+\gamma_{b0}e^{-2\sigma_0 L}}{1-\gamma_{b0}e^{-2\sigma_0 L}}\right). \tag{50}$$

This equation is, as expected, the well-known expression for the thermal-wave field at the surface of a solid of constant thermophysical parameters (diffusivity α_0 and conductivity k_0) and thickness L, surrounded by air (front surface) and supported by a semi-infinite backing material of (also) constant thermophysical parameters (α_b,k_b); see, for instance, Ref. 1, Eq. (27).

6. No upper layer: $L=0$

Using the definitions

$$\frac{1+\gamma_{bL}}{1-\gamma_{bL}}=\frac{R_b}{R_L},\qquad \frac{1+\gamma_{b0}}{1-\gamma_{b0}}=R_b, \tag{51}$$

and Eq. (48), it can be shown that, in the limit $L\to 0$, the general field Eq. (40) now reduces to

$$T(0,0,\omega)=R_b\Theta_0(\omega)=\frac{Q_0}{2k_b\sigma_b}=T_b(0,\omega), \tag{52}$$

i.e., it yields the expression for the surface value of the thermal-wave field in the semi-infinite solid of thermophysical parameters equal to those of the substrate. This is as expected since, when $L=0$, the geometry is that of a single-layer, homogeneous semi-infinite solid: the substrate.

7. $q\to+\infty$

In this limit the profile is flat with $\alpha(x)=\alpha_L$ except at $x=0$, where it is equal to α_0. This requires that

$$T(0,q\to\infty,\omega)\to\frac{Q_0}{2k_L\sigma_L} \tag{53}$$

except when $\omega\to\infty$.

It can be shown that in this limit $H(L)\to\sigma_L L$. Therefore Eq. (41) yields $\sigma_L J_L\to 0$. Using these results from the updated version [substituting for b from Eq. (48) and d from Eq. (49)] of Eq. (40), it can be easily verified that to satisfy the condition in Eq. (53) one must set

$$c=1. \tag{54}$$

8. $q\to-\infty$

In this limit the profile is flat with $\alpha(x)=\alpha_0$ except at $x=L$, where it is equal to α_L. This requires that

$$T(0,q\to-\infty,\omega)\to\frac{Q_0}{2k_0\sigma_0}\sim\Theta_0(\omega). \tag{55}$$

In the limit $q\to-\infty$ it can be shown that $H(L)\to\sigma_0 L$. Therefore

$$\sigma_L J_L\to(\sigma_L-\sigma_0)L. \tag{56}$$

Substituting Eqs. (55) and (56) in the latest version ($c=1$) of Eq. (40) yields

$$de^{-H(L)}=\left[\left(\frac{1+\gamma_{b0}e^{-2\sigma_0 L}}{1-\gamma_{b0}e^{-2\sigma_0 L}}-R_L\left(\frac{1+\gamma_{bL}e^{-2\sigma_L L}}{1-\gamma_{bL}e^{-2\sigma_L L}}\right)\frac{e^{-[H(L)-\sigma_0 L]}}{(R_L-1)(e^{-(\sigma_L-\sigma_0)L}-1)\left[1-\frac{R_L}{R_b}\left(\frac{1+\gamma_{bL}}{1-\gamma_{bL}e^{-2\sigma_L L}}\right)e^{-\sigma_L L}\right]}\right.$$
$$\left.+e^{-[\sigma_0 L+H(L)]}-e^{-[H(L)-\sigma_0 L]}\right]. \tag{57}$$

Then the final expression for $T(0,\omega)$ takes the form

$$T(0,\omega)=\Theta_0(\omega)(R_L-1)(e^{-\sigma_L J_L}-1)(1+de^{-H(L)}-e^{-2H(L)})\left[1-\frac{R_L}{R_b}\left(\frac{1+\gamma_{bL}}{1-\gamma_{bL}e^{-2\sigma_L L}}\right)e^{-\sigma_L L}\right]+\Theta_0(\omega)R_L\left(\frac{1+\gamma_{bL}e^{-2\sigma_L L}}{1-\gamma_{bL}e^{-2\sigma_L L}}\right), \tag{58}$$

where $de^{-H(L)}$ is given by Eq. (57). Therefore, the general Eq. (58) satisfies all the physical limiting requirements for the thermal-wave field at the surface of an exponentially inhomogeneous material of finite thickness on a homogeneous substrate.

The foregoing derivation assumed a decreasing thermal diffusivity profile. It can be shown numerically from simulated data that, by defining $\sigma_L J_L$ with a positive magnitude, Eq. (58) satisfies both increasing and decreasing profiles. That is,

$$\sigma_L J_L=\sigma_L|L-A|, \tag{59}$$

where

$$A=\left[\frac{1-e^{-qL}}{1-\sqrt{(\alpha_0/\alpha_L)}e^{-qL}}\right]\left[L-\frac{1}{2q}\ln\left(\frac{\alpha_0}{\alpha_L}\right)\right]. \tag{60}$$

This can be shown from Eqs. (4), (32), and (41).

Validity of Eq. (58). Equation (58) is valid for arbitrary exponential (in principle) profiles $\alpha_s(x)$, wherein at every frequency ω_i the surface ac temperature response of a material structure gives two data channels, namely, amplitude and phase. In practice, the validity of Eq. (58) is much more general than the assumed exponential profile of Eq. (11a), as it is possible to update the fitted exponential profile at each experimental angular frequency ω_i through a new pair of values (α_0,q) or (α_L,q). Here, the thickness L and the thermal properties of the substrate are assumed to be known parameters. Thus entirely arbitrary depth profiles may be reconstructed by numerically determining the optimal pair of

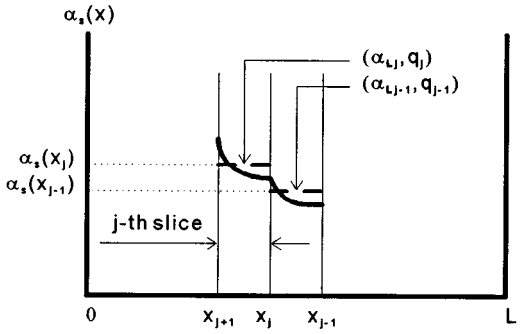

FIG. 2. A graph illustrating the method of determining the thermal diffusivity profile by virtual ''slicing.''

the foregoing values so that the profile sought locally results in the experimentally observed thermal-wave signal amplitude and phase data. In what follows, the symbol α_L will be used in lieu of either α_0 or α_L, unless stated otherwise. Where all system parameters are known except for the pair (α_L, q) in Eq. (11a), the pair of local values (α_L, q) may be determined from two data values, amplitude and phase, at modulation frequency ω_j. In computations, frequency ω_j is decremented from $\omega_j \rightarrow \omega_{j+1}$ and a new parameter pair will be calculated $(\alpha_L, q)_j \rightarrow (\alpha_L, q)_{j+1}$. Therefore at each ω_j a system of two equations with two unknown parameters may be solved. The solution yields $(\alpha_L, q)_j$ and these values are inserted in Eq. (11a) to obtain $\alpha_s(x_j)$, where x_j represents the root-mean-square thermal probe depth in the solid at frequency ω_j, determined in terms of the local thermal diffusion length $\mu_j(x_j)$.

Therefore the present method for obtaining the inverse thermal wave fits into every material ''slice,'' an exponential function of the type of Eq. (11a) for $\alpha_s(x_j)$. The thickness of that slice depends on $\Delta\omega_j = \omega_j - \omega_{j+1}$ as shown in Fig. 2. The depth of the slice depends on the frequency ω_j and $\alpha_s(x_j)$.

Based on the amplitude and phase data at a given ω_j the solution to the numerical algorithm described below yields the best fit values $(\alpha_L, q)_j$ at the local slice (j) which, in turn, determines a local diffusivity value in best agreement with the photothermal data. Therefore as already discussed, the profile assumed in Eq. (11a) is only used for convenience and analytical consistency. The true depth profile is built up by individual slice profiles, each of which is best fitted to a local Eq. (11a). Any other profile $\alpha_s(x)$ would be just as acceptable, provided the integral $H(L)$ can be calculated. The exponentially decreasing profile has the advantage of superior sensitivity to local changes in α_s values that can be easily accommodated as changes in q, as compared to algebraic profiles.

Accordingly, any arbitrary $\alpha_s(x)$ profile can therefore be reconstructed by ''slicing'' inhomogeneous layers into local thin layers in which the local diffusivity value coincides with the value of $\alpha_s(x)$ given by Eq. (11a) at that depth.

III. COMPUTATIONAL AND NUMERICAL METHODOLOGY

The surface temperature response to the incident light beam on the investigated system or sample is normalized by the surface temperature response to the same beam of the same frequency on a semi-infinite homogeneous material (reference). This gives for each frequency a data pair, namely, amplitude ratio and phase difference between sample and reference. The normalizing procedure is necessary for the correct accounting of all frequency dependencies in the apparatus other than that due to the investigated sample (Fig. 1) that is the instrument transfer function. Theoretical values of the data pair are calculated by Eq. (58).

$$|M(\omega)|e^{i\Delta\phi(\omega)} = \text{right-hand side of Eq. (58).} \qquad (61)$$

$|M(\omega)|$ is the amplitude ratio and $\Delta\phi(\omega)$ is the phase difference at angular frequency ω.

The analytical separation of magnitude and phase of Eq. (58) would be a difficult process. Also, finding an analytical solution to Eq. (61) is not possible. Therefore a numerical solution was obtained by using the following steps.

Step one is to initialize theoretical amplitudes. If the experimental data amplitude ratio $|M_{\text{exp}}(\omega_j)|$ differs from the theoretical one, one of the ratios (for numerical reasons the data values are chosen) must be multiplied by a ''scaling constant'' that is calculated as a ratio between theoretical and experimental data amplitudes for the highest frequency, using initial values of $\alpha_{L(1)}$ and $q_{(1)}$. Since the initial values of $\alpha_{L(1)}$ and $q_{(1)}$ for the highest frequency are unavailable, an approximate set of initial values can be obtained by fitting the extrema of the data[14] to theoretically simulated data corresponding to a single exponential profile [given by Eq. (11a)]. Then the following steps are executed. If no satisfying solution is found $\alpha_{L(1)}$ is increased by 1%.

Step two is to fine-tune the scaling constant. In order to eliminate data error for the highest frequency that are caused by improper α_0, $\alpha_{L(1)}$, and $q_{(1)}$ values, roundoff errors, and inhomogeneities in the reference sample, and most importantly the effect of reflectivity and/or emissivity of the surfaces of both the reference and the sample, a scale constant is used that is in the range of $\pm 5\%$ of the initial one. The process is started with the lower value and then step three is applied. If no satisfactory solution is found, the scaling constant is increased by 1%. Combined with the range of initial values of $\alpha_{L(1)}$ of step one by which the scaling constant was determined, all practical possibilities of data amplitudes are tried.

Step three is to search for local $\alpha_{L(j)}$ and $q_{(j)}$. In this numerical search for solutions to Eq. (58), the search for (α_L, q) is chosen over a (α_0, q) search because a (α_L, q) search finds solutions much faster and is tolerant to noise in the data. To be able to calculate the thermal diffusivity $\alpha_s(x)_{(j)}$ and depth $x_{(j)}$ corresponding to frequency $\omega_{(j)}$ one has to find unknown parameters $\alpha_{L(j)}$ and $q_{(j)}$. A customized two-dimensional Broyden method[15] was used. The procedure was customized to avoid run time errors and singularities in Broyden's two-dimensional line search procedure so that the procedure may be used in conjunction with Eq. (58). The method looks for $\alpha_{L(j)}$ and $q_{(j)}$ to satisfy the minimum con-

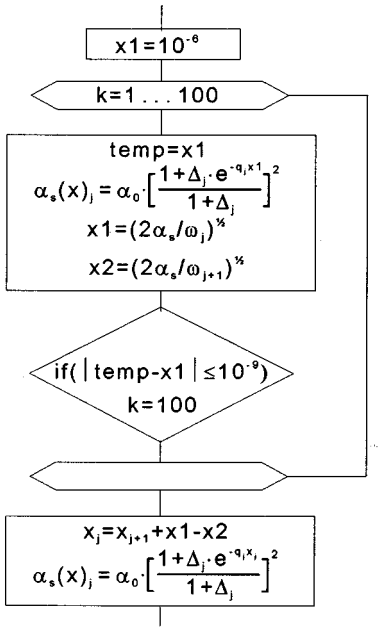

FIG. 3. Flow chart showing the algorithm of determining the thermal diffusivity $\alpha_s(x)_j$ and the corresponding depth x_j. Here $j=1$ represents the highest frequency.

ditions $|M_{\exp}(\omega_j)|-|M(\omega_j)|=0$ and $\Delta\phi_{\exp}(\omega_j)-\Delta\phi(\omega_j)=0$ for each angular frequency ω_j. The program was written in C++, so that library functions could be used to separate real and imaginary parts of the right-hand side of Eq. (58) to calculate $|M(\omega_j)|$ and $\Delta\phi(\omega_j)$. The procedure starts with the highest frequency ω_1. If no solution is found for some of the frequencies, the scaling constant is increased by 1% and the procedure returns to step two above. If the scaling constant reaches the upper boundary of the allowed range and still no solution has been found for each of the frequencies, the procedure returns to step one where the initial $\alpha_{L(j)}$ is increased by 1%. When solutions are found for a specified number of frequencies, the procedure advances to step four.

Step four is the calculation of $\alpha_s(x)_{(j)}$ and depth $x_{(j)}$. After all local values of $\alpha_{L(j)}$ and $q_{(j)}$ are known, the thermal diffusivity profile of the sample is calculated. Starting at the highest frequency, $\omega_{(1)}$, where a solution was found, the corresponding $\alpha_{L(1)}$ and $q_{(1)}$ are used for determining the thermal diffusivity and the shallowest depth using the algorithm or schematic diagram shown in Fig. 3. In this algorithm a smooth continuity is applied wherein if $\alpha_s(x)_{(j)}$ significantly differs from the neighboring $\alpha_s(x)_{(j+1)}$, the scaling constant is increased by 1%, and the program returns to step two. If depth $x_j \geqslant L$ is reached, no other frequency is needed and the program plots the thermal diffusivity in the desired layer. This entire procedure takes a few seconds on a PC with 100 MHz Pentium provided that a reasonable set of initial parameters is given.

By choosing a numerically very large value for the thickness L, the same software program can be used to perform inversions for semi-infinite samples. Here, since $\alpha_\infty(=\alpha_L)$ is generally known (a homogeneous bulk material), it is more convenient to search for α_0.

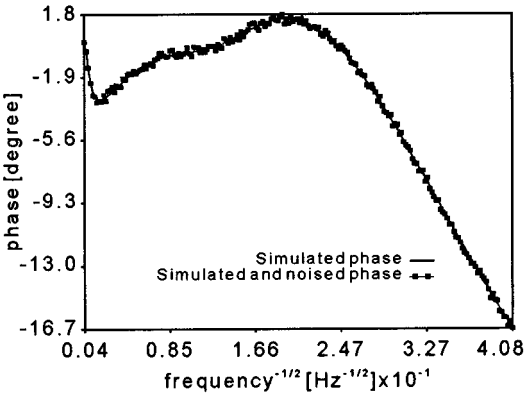

FIG. 5. A graph illustrating the phase frequency dependence for the simulated profile of Fig. 4. The solid line represents original data. The jagged line represents the data with 0.3° random noise added.

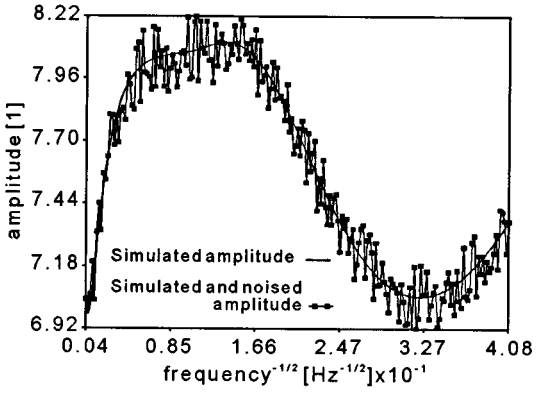

FIG. 4. A graph illustrating the amplitude frequency dependence for a simulated exponential diffusivity depth profile. The solid line represents original data. The jagged line represents the data with 2% random noise added.

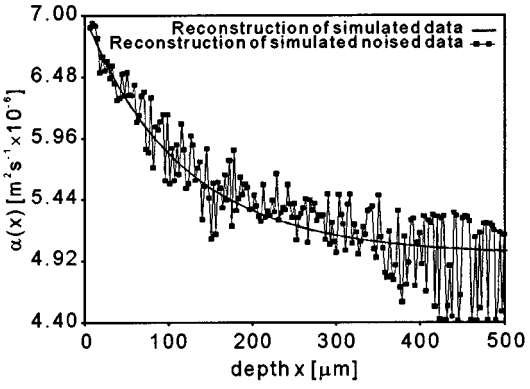

FIG. 6. A graph illustrating the depth dependence of the thermal diffusivity reconstructed profiles from the data shown in Figs. 5 and 6, without extraneous noise (solid line), and with added random noise to these data (2% noise to the amplitude and 0.3° noise to the phase). The original input diffusivity depth profile coincides with the noiseless reconstructed profile.

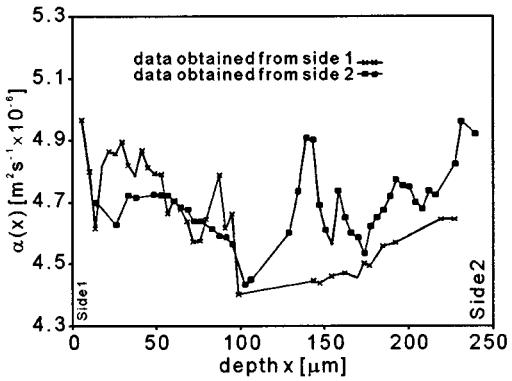

FIG. 7. Reconstructed thermal diffusivity profiles obtained from both sides of a machined stainless steel plate 250 μm thick.

IV. RESULTS FROM SIMULATED AND EXPERIMENTAL DATA

To test the above reconstruction procedure, we used simulated data for the forward problem generated with an exponentially decreasing profile of the type of Eq. (11a), with random noise added to it. Figures 4 and 5 show the simulated data and the data with added random noise (2% to amplitude and 0.3° to phase) corresponding to the profile of Eq. (11a) with $q=3000\ \mathrm{m}^{-1}$, $\alpha_0=7\times10^{-6}\ \mathrm{m}^2\,\mathrm{s}^{-1}$, $\alpha_L=5\times10^{-6}\ \mathrm{m}^2\,\mathrm{s}^{-1}$, $L=500\ \mu$m, with air ($\alpha_b=22\times10^{-6}\ \mathrm{m}^2\,\mathrm{s}^{-1}$, $k_b=26\times10^{-3}\ \mathrm{W\,m}^{-1}\,\mathrm{K}^{-1}$) as the substrate. This amounts to the simulation of a free standing steel plate.

Figure 6 shows the corresponding reconstructed profile from the noisy data using the above computational procedure as well as the reconstructed noiseless profile and the original input profile. This result shows that the reconstruction algorithm has sufficient insensitivity to noise and it reconstructs the original profile quite well. It should be pointed out that the noise levels assumed here are worse than the experimentally attainable levels that are reported in a forthcoming article.[16]

Figure 7 shows the reconstructed profiles obtained from the experimental data taken from both sides of a machined stainless steel plate 250 μm thick. This sample could be treated as a layer of thickness $L(=250\ \mu\mathrm{m})$ on a homogeneous substrate (air). The experimental procedure is described elsewhere[8] and will not be repeated here. This reconstruction demonstrates the precision of this technique, within the experimental noise limits, in reconstructing an essentially homogeneous layer. The increase in thermal diffusivity towards the surfaces may be due to the machining process causing tensile damage, manifested as a region of decreased material density.

V. CONCLUSIONS

The Hamilton–Jacobi formulation of the thermal-wave problem together with the concept of linear superposition of solutions of the heat diffusion boundary-value problem was found to provide a generalized expression for the surface ac temperature of an inhomogeneous opaque solid on a homogeneous substrate that could also be used for a continuously inhomogeneous semi-infinite solid. Using this expression, a successful inversion procedure to reconstruct thermal diffusivity profiles was described. Its sufficient insensitivity to artificial noise in the data was also confirmed. This method could be used to analyze the level of homogeneity of coatings on substrate or free standing thin layers as shown by the steel plate example. A more detailed description of the experimental results with several examples will be presented in a forthcoming article.[16]

ACKNOWLEDGMENT

The support of the Manufacturing Research Corporation of Ontario (MRCO) is gratefully acknowledged.

[1] G. Busse and H. G. Walther, *Progress of Photothermal and Photoacoustic Science and Technology*, edited by A. Mandelis (Elsevier, New York, 1992), Vol. 1, pp. 205–298.
[2] H. J. Vidberg, J. Jarrinen, and D. O. Riska, Can. J. Phys. **64**, 1178 (1986).
[3] J. Jaarinen and M. Luukkala, J. Phys. (Paris) **C6-44**, 503 (1983).
[4] A. Mandelis, S. B. Peralta, and J. Thoen, J. Appl. Phys. **70**, 1761 (1991).
[5] A. Mandelis, J. Math. Phys. (N.Y.) **26**, 2676 (1985).
[6] A. Mandelis, E. Schoubs, S. B. Peralta, and J. Thoen, J. Appl. Phys. **70**, 1771 (1991).
[7] T.-C. Ma, M. Munidasa, and A. Mandelis, J. Appl. Phys. **71**, 6029 (1992).
[8] M. Munidasa, T. C. Ma, A. Mandelis, S. K. Brown, and L. Mannik, Mater. Sci. Eng. A **159**, 111 (1992).
[9] C. Glorieux, J. Fivez, and J. Thoen, J. Appl. Phys. **73**, 684 (1993).
[10] F. Funak, A. Mandelis, and M. Munidasa, J. Phys. (Paris) III **C7-4**, 95 (1994).
[11] J. Fivez and J. Thoen, J. Appl. Phys. **75**, 7696 (1994).
[12] T. T. N. Lan, U. Seidel, and H. G. Walther, J. Appl. Phys. **77**, 4739 (1995).
[13] T. T. N. Lan, U. Seidel, H. G. Walther, G. Goch, and B. Schmitz, J. Appl. Phys. **78**, 4108 (1995).
[14] J. Fivez and J. Thoen, J. Appl. Phys. **79**, 2225 (1996).
[15] W. H. Press, S. A. Teukolsky, W. T. Vetterling, and B. P. Flannery, *Numerical Recipes in C*, 2nd ed. (Cambridge University Press, Cambridge, 1992), p. 398.
[16] M. Munidasa, F. Funak, A. Mandelis, and S. B. Peralta (unpublished).